Linear Frequency Domain Reduced Order Modelling of Aerofoil Gust Response

Amir K. Bagheri[1], Dorian P. Jones[2], Ann L. Gaitonde[3]
University of Bristol, Bristol, England BS8 1TR, United Kingdom

A method for constructing reduced order models of an aerofoil subject to gusts is presented. The method is based on subspace system identification in the frequency domain in order to obtain a model which retains the dynamic information of the original system, while having a comparatively smaller dimension. The gust is prescribed through the domain using the split velocity method to obtain the system frequency response. This is used to find the state matrices of the reduced system. By prescribing a series of 1-cosine gusts, it is shown that the reduced system obtained agrees well with the original system.

Nomenclature

A, B, C, D	=	continuous state space matrices
$\hat{A}, \hat{B}, \hat{C}, \hat{D}$	=	discrete state space matrices
$\Delta\alpha_{eff}$	=	effective change in angle of attack due to gust
e_g	=	component of total energy due to gust
$\boldsymbol{F}, \boldsymbol{G}, \breve{\boldsymbol{F}}, \breve{\boldsymbol{G}}$	=	flux vectors
$G_d(z)$	=	discrete system transfer function
k_{red}	=	reduced frequency
λ	=	gust length
M	=	$N_\omega - 1$
N_ω	=	number of frequency response samples
N_r	=	size of reduced order model
ω	=	gust excitation frequency
ω_k	=	continuous input frequency
ω_k^d	=	$\omega_k \times T$
$\boldsymbol{Q}$	=	$[\rho \quad \rho u \quad \rho v \quad \rho e]^T$
s	=	Laplace variable
s_m , s_e	=	gust source term functions
t	=	time
T	=	sampling period
$\boldsymbol{u}$	=	discrete input vector
$\bar{u}, \bar{v}$	=	steady state velocity components
u_g, v_g	=	gust velocity components
$\hat{u}, \hat{v}$	=	perturbation velocity components
u_{ref}	=	freestream velocity
$\tilde{u}, \tilde{v}$	=	$u - u_g$, $v - v_g$
$v_{g_{max}}$	=	gust amplitude
$\boldsymbol{x}$	=	state vector
x_0	=	gust starting position at time zero
x_t , y_t	=	grid speeds
$\boldsymbol{y}$	=	output vector
z	=	Z-transform variable

I. Introduction

THE evaluation of unsteady loads plays a critical role in civil aircraft design and manufacture. In most of the preliminary and final design stages of an aircraft, many hours of computational effort is required in order to fully test for all possible flight cases and expected scenarios. In addition to this, many flight tests are also carried out to ensure the safe operation of the aircraft under various conditions. The study of the effects of gusts and external excitations on the aircraft forms a critical part of safety validation tests, and plays an integral role in fatigue calculations and airframe lifetime estimations. There is a growing need for developing computational models which could accurately and effectively predict the loads from the full aircraft in a fraction of the time, which is the main motivation behind Reduced Order Modelling.

In this study, a method has been developed to create Reduced Order Models (ROMs) to predict the response of a 2D aerofoil to external gusts. The ROM allows the effects of the gust on the aerofoil to be studied without needing to

[1] Research Associate, Aerospace Department, Aerospace Engineering, Queen's Building, University Walk.
[2] Senior Lecturer, Aerospace Department, Aerospace Engineering, Queen's Building, University Walk.
[3] Senior Lecturer, Aerospace Department, Aerospace Engineering, Queen's Building, University Walk.

run time domain simulations, which saves considerable computational time. Moreover, for any dynamic system under study only one ROM is needed to model the output of the system to any arbitrary input. This implies that there is no need to run multiple time domain computational fluid dynamics (CFD) based simulations, allowing more computational effort to be directed towards running CFD simulations of more critical cases.

Before the ROM is constructed the accurate simulation of the gust is developed using the Split Velocity Method (SVM) [1], where the velocity distribution is decomposed so that the prescribed onset gust velocity is treated separately. This involves no approximation just the rearrangement of the flow equations.

The SVM is coded as a modified version of the Euler equations on a moving grid, with the addition of source terms dependant on the gradients of the prescribed onset gust. Harmonic gusts are prescribed to find the complex frequency response of the system. The development of SVM to analyse harmonic gusts is a novel approach incorporated in this work. The frequency response obtained is subsequently used in a system identification algorithm to construct a lower-dimensional system which exhibits the same dynamic characteristics as the original system.

The ROMs obtained have been tested against the results from the same linearised CFD code in the time domain, by prescribing a series of 1-cosine gusts and comparing the outputs from both systems. Good agreements were observed between the two approaches, especially at lower excitation frequencies, which is the main operational regime of a civil airliner.

It is suggested that, once fully developed, the ROM could be extended into a nonlinear viscous model of a full aircraft, providing significant savings of time and computational resources over full order simulations.

II. Background

A. Moving Grid Equations

The moving grid equations are briefly introduced in this section to show their similarity to the SVM equations.
The non-dimensional 2D unsteady Euler equations in conservative differential form are:

$$\frac{\partial}{\partial t}\boldsymbol{Q} + \frac{\partial}{\partial x}\boldsymbol{F} + \frac{\partial}{\partial y}\boldsymbol{G} = 0 \tag{1}$$

Where

$$\boldsymbol{Q} = \begin{bmatrix} \rho \\ \rho u \\ \rho v \\ \rho e \end{bmatrix} \quad , \quad \boldsymbol{F} = \begin{bmatrix} \rho u \\ \rho u^2 + p \\ \rho uv \\ u(\rho e + p) \end{bmatrix} \quad , \quad \boldsymbol{G} = \begin{bmatrix} \rho v \\ \rho uv \\ \rho v^2 + p \\ v(\rho e + p) \end{bmatrix}$$

Pressure is related to the flow variables by the equation of state:

$$p = \rho(\gamma - 1)(e - \frac{1}{2}(u^2 + v^2)) \tag{2}$$

The above Euler equations are actually solved in the following integral form for a moving mesh:

$$\frac{\partial}{\partial t}\iint_{\Omega}\boldsymbol{Q}\,\partial x\,\partial y + \int_{\partial\Omega}\left(\breve{\boldsymbol{F}}\,\partial y - \breve{\boldsymbol{G}}\,\partial x\right) = 0 \tag{3}$$

Where x_t and y_t are the grid speeds and the modified flux matrices for a moving mesh are given by:

$$\breve{\boldsymbol{F}} = \begin{bmatrix} \rho(u - x_t) \\ \rho u(u - x_t) + p \\ \rho v(u - x_t) \\ \rho e(u - x_t) + pu \end{bmatrix} \quad , \quad \breve{\boldsymbol{G}} = \begin{bmatrix} \rho(v - y_t) \\ \rho u(v - y_t) \\ \rho v(v - y_t) + p \\ \rho e(v - y_t) + pv \end{bmatrix}$$

The grid position and speeds must be evaluated at each time step and a geometric conservation law (GCL) must be solved to correctly account for the mesh movement [2].

B. Split Velocity and Field Velocity Method

Instead of using the moving grid equations to find the response of the aerofoil to sinusoidal pitch excitations, the grid could be kept fixed and a sinusoidal gust could be prescribed. This can be done by starting with the Euler equations on a fixed grid, and decomposing the velocities into prescribed gust velocity and the remaining velocity component. This is known as the Split Velocity Method [1]. Compared to other unsteady gust modelling techniques such as the Farfield Boundary Condition (FBC) method, where the gust is prescribed by way of the outer domain boundary conditions, SVM does not require a very fine mesh to prevent the dissipation of the gust. Furthermore, it fully accounts for the mutual interactions between the gust and the aerofoil. This is in contrast to the Field Velocity Method (FVM) [3,4] which neglects the additional gust source terms that exist in the SVM equations. In both methods the grid time metrics are modified to physically introduce the motion of the gust throughout the computational domain, without actually moving the grid itself. The resulting equations are very similar to the moving mesh equations given previously, which has the advantage that any existing moving mesh solver requires only minor modifications to model gusts using the FVM or SVM approaches. A brief derivation of the SVM equations is given below:

Starting from Eq. (1) the velocity and energy terms are decomposed as follows:

$$u = \tilde{u} + u_g \qquad v = \tilde{v} + v_g \qquad e = \tilde{e} + e_g \tag{4}$$

Where u_g and v_g are the prescribed gust components. Substituting the velocities into Eq. (2), the total energy can be split as follows:

$$e = \frac{p}{\rho(\gamma-1)} + \frac{1}{2}(u^2+v^2) = \underbrace{\frac{p}{\rho(\gamma-1)} + \frac{1}{2}(\tilde{u}^2+\tilde{v}^2)}_{\tilde{e}} + \underbrace{(\tilde{u}u_g + \tilde{v}v_g) + \frac{1}{2}({u_g}^2 + {v_g}^2)}_{e_g} \tag{5}$$

Substituting these new components into Eq. (1) and separating the applied gust from the rest of the solution gives:

$$\frac{\partial}{\partial t}\begin{bmatrix}\rho\\ \rho\tilde{u}\\ \rho\tilde{v}\\ \rho\tilde{e}\end{bmatrix} + \frac{\partial}{\partial x}\begin{bmatrix}\rho(\tilde{u}+u_g)\\ \rho\tilde{u}(\tilde{u}+u_g)+p\\ \rho\tilde{v}(\tilde{u}+u_g)\\ \rho\tilde{e}(\tilde{u}+u_g)+p\tilde{u}\end{bmatrix} + \frac{\partial}{\partial y}\begin{bmatrix}\rho(\tilde{v}+v_g)\\ \rho\tilde{u}(\tilde{v}+v_g)\\ \rho\tilde{v}(\tilde{v}+v_g)+p\\ \rho\tilde{e}(\tilde{v}+v_g)+p\tilde{v}\end{bmatrix} + \begin{bmatrix}0\\ s_m(u_g)\\ s_m(v_g)\\ s_e(u_g,v_g)\end{bmatrix} = 0 \tag{6}$$

Where the source terms are:

$$s_m(.) = \rho\left\{\frac{\partial .}{\partial t} + (\tilde{u}+u_g)\frac{\partial .}{\partial x} + (\tilde{v}+v_g)\frac{\partial .}{\partial y}\right\}$$
$$s_e(u_g,v_g) = \tilde{u}s_m(u_g) + \tilde{v}s_m(v_g) + p\left(\frac{\partial u_g}{\partial x} + \frac{\partial v_g}{\partial y}\right) \tag{7}$$

The pressure remains unchanged by these substitutions and is given by:

$$p = \rho(\gamma-1)\left(\tilde{e} - \frac{1}{2}(\tilde{u}^2+\tilde{v}^2)\right) \tag{8}$$

It can be seen from Eqs. (3) and (6) that the SVM equations are equivalent to the Euler equations on a moving mesh, with the grid speeds equal to minus the gust speeds, and the addition of extra source terms.

C. Linearization of SVM

By decomposing the flow variables into the sum of a steady and a time-varying component and assuming that the product of the perturbations is negligible, the nonlinear SVM equations can be linearised:

$$\rho = \bar{\rho} + \hat{\rho} \qquad \tilde{u} = \bar{u} + \hat{u} \qquad \tilde{v} = \bar{v} + \hat{v} \qquad \tilde{e} = \bar{e} + \hat{e} \qquad p = \bar{p} + \hat{p} \tag{9}$$

The linearised source terms become:

$$s_m(.) = \bar{\rho}\left\{\frac{\partial .}{\partial t} + \bar{u}\frac{\partial .}{\partial x} + \bar{v}\frac{\partial .}{\partial y}\right\}$$
$$s_e(u_g, v_g) = \bar{u}s_m(u_g) + \bar{v}s_m(v_g) + \bar{p}(\frac{\partial u_g}{\partial x} + \frac{\partial v_g}{\partial y}) \quad (10)$$

The linear equations are solved in integral form on a fixed mesh, using a dual-time version of Jameson's cell-centered finite volume scheme [5].

The linear time domain (LTD) SVM solver can then be used to simulate a vertical gust given by a travelling sine wave in order to obtain the frequency response of the system. This gust is defined by:

$$v_g = v_{g_{max}} \sin\left(\frac{2\pi}{\lambda}(x - u_{ref}t)\right) \quad (11)$$

Where λ is the gust wavelength, and u_{ref} is the reference freestream velocity. Note that the gust propagation does not need to start from the far-stream boundary since the steady state response is unaffected by the gust's starting position.

D. Frequency Domain Representation of SVM

Finding the frequency response of the system by running multiple time domain simulations is impractical and highly inefficient, since many time-intensive simulations need to be completed at different excitation frequencies to obtain the steady state response. An alternative and more efficient approach would be to solve the equations in the frequency domain, by taking the flow variables as being harmonic in time. Since the system is linear, for a harmonic input the output of the system will also be harmonic and at the same frequency; it will only differ in magnitude and phase.

The unsteady perturbations are represented as their first Fourier harmonic:

$$\hat{\rho} = \hat{\rho}^c e^{i\omega t} \quad \hat{u} = \hat{u}^c e^{i\omega t} \quad \hat{v} = \hat{v}^c e^{i\omega t} \quad \hat{p} = \hat{p}^c e^{i\omega t} \quad (12)$$

Where the superscript c denotes a complex variable, and ω is the response frequency, which for a linear system equals the excitation frequency. For the sinusoidal gust given by Eq. (11), the excitation frequency equals:

$$\omega = \frac{2\pi}{\lambda}u_{ref} \quad (13)$$

The gust source terms in the SVM solver also need to be re-evaluated for application in the linear frequency domain (LFD) code. Noting that the gust is purely vertical and therefore $u_g = \frac{\partial v_g}{\partial y} = 0$ the source terms simplify to:

$$s_m(u_g) = 0$$
$$s_m(v_g) = \bar{\rho}\left\{\frac{\partial v_g}{\partial t} + \bar{u}\frac{\partial v_g}{\partial x}\right\} \quad (14)$$
$$s_e(v_g) = \bar{v}s_m(v_g)$$

Equation (11) also needs to be converted to exponential form:

$$v_g = {v_g}^c e^{i\omega t} + {v_g}^{c^*} e^{-i\omega t}$$
$${v_g}^c = \frac{1}{2}\left[v_{g_{max}} \sin\left(\frac{2\pi}{\lambda}x\right) + iv_{g_{max}} \cos\left(\frac{2\pi}{\lambda}x\right)\right] \quad (15)$$

Where the asterisk denotes the complex conjugate. Substituting only the positive frequency from the above equation into Eq. (14) the linear source terms in the frequency domain can be derived. Note that since the system is linear the principal of superposition holds, meaning that the positive and negative frequencies from Eq. (15) can be prescribed separately. It should be further noted that since the negative frequency input is the complex conjugate of the positive frequency, the response obtained will simply be the complex conjugate of that from the positive input. Hence only the positive frequency solution must be found using the LFD solver. Noting that the exponential terms naturally drop out of the LFD equations, the gust source terms in the frequency domain become:

$$\text{Real} \begin{cases} {s_m}^{Re}(v_g) = \bar{\rho}\, v_{g_{max}} k_{red}(\bar{u} - u_{ref}) \cos\left(\frac{2\pi}{\lambda}x\right) \\ {s_e}^{Re}(v_g) = \bar{v}\, {s_m}^{Re}(v_g) \end{cases}$$

$$\text{Imaginary} \begin{cases} {s_m}^{Im}(v_g) = \bar{\rho}\, v_{g_{max}} k_{red}(u_{ref} - \bar{u}) \sin\left(\frac{2\pi}{\lambda}x\right) \\ {s_e}^{Im}(v_g) = \bar{v}\, {s_m}^{Im}(v_g) \end{cases} \tag{16}$$

Where k_{red} is the reduced frequency per unit chord, defined as:

$$k_{red} := \frac{\omega}{2u_{ref}} = \frac{\pi}{\lambda} \tag{17}$$

The source terms can be written in integral form and evaluated analytically over each cell.

Inspecting the LFD equations, the steady state gain at zero frequency and the limit of the response magnitude and phase as the excitation frequency tends to +∞ can be identified. At zero frequency, Eq. (15) becomes purely imaginary, and the source terms vanish. For this input, the phase of the output equals 0, while the magnitude equals the output of a steady simulation at an angle of attack equivalent to the effective change in angle of attack due to the gust:

$$\Delta\alpha_{eff} = \tan^{-1}\left(\frac{v_{g_{max}}}{u_{ref}}\right) \tag{18}$$

As the frequency tends to +∞, the source terms tend to 0. It can be shown that the flow equations become purely imaginary at very large frequencies, implying that the system response will be out of phase with the input.

E. System Identification

The objective of the frequency domain system identification described by McKelvey et al. [6] is to identify a state-space model given samples of the frequency response function. A key stage in the identification of said system is using a truncated singular value decomposition (SVD) for the extraction of a low-dimensional subspace, allowing a Reduced Order Model (ROM) of the original system to be created. In order to find a ROM of the 2D aerofoil-gust system under study, the LFD solver was run with a range of harmonic inputs at various frequencies. By dividing the output aerofoil lift coefficient by the magnitude of the gust input, and by finding the phase difference between the input and output, the system frequency response was found. The frequency response is subsequently used in the system identification.

The state-space equation for a Multiple-Input & Multiple-Output (MIMO), Linear Time-Invariant (LTI) continuous system is:

$$\begin{aligned} \dot{\boldsymbol{x}} &= A\boldsymbol{x} + B\boldsymbol{u} \\ \boldsymbol{y} &= C\boldsymbol{x} + D\boldsymbol{u} \end{aligned} \tag{19}$$

Where *A, B, C,* & *D* are the continuous system matrices. For a discrete system this becomes:

$$\begin{aligned} \boldsymbol{x}(n+1) &= \hat{A}\boldsymbol{x}(n) + \hat{B}\boldsymbol{u}(n) \\ \boldsymbol{y}(n) &= \hat{C}\boldsymbol{x}(n) + \hat{D}\boldsymbol{u}(n) \end{aligned} \tag{20}$$

Where $\hat{A}, \hat{B}, \hat{C}$ & $\hat{D}$ are the discrete system matrices. $\boldsymbol{x} \epsilon \mathbb{R}^{n\times 1}$ is the state vector, $\boldsymbol{u} \epsilon \mathbb{R}^{r\times 1}$ is the input vector, and $\boldsymbol{y} \epsilon \mathbb{R}^{m\times 1}$ is the output vector [7]. Taking a continuous harmonic input with frequency ω_k, and sampling it at a period of T seconds, the equivalent discrete input can be found:

$$\boldsymbol{u}(n) = \tilde{u}_k e^{i\omega_k nT} = \tilde{u}_k e^{i\omega_k^d n} \tag{21}$$

Where ω_k^d has been defined as the continuous-time excitation frequency ω_k multiplied by the sampling period T.

Inputting the above into Eq. (20), and similarly assuming discrete harmonic input and output, it can be shown that the frequency response function for the discrete LTI system can be written as:

$$G_d(\omega_k^d) = \hat{C}\left(e^{i\omega_k^d} I - \hat{A}\right)^{-1} \hat{B} + \hat{D} \tag{22}$$

Comparing the above to the discrete system transfer function, which is obtained by applying the Z transform to Eq. (20) and solving for the relationship between the input and the output, it can be shown that the two equations are equal if the discrete system poles are evaluated on the unit circle, namely:

$$z = e^{i\omega_k^d} \tag{23}$$

The discrete time transfer function is given by:

$$G_d(z) = \hat{C}(zI - \hat{A})^{-1}\hat{B} + \hat{D} \tag{24}$$

It can be shown that by approximating the integral of the continuous state space equations from time *nT to (n+1)T* using the trapezium rule, and applying the Z-transform to the result to obtain the discrete transfer function, the discrete and continuous transfer functions are equivalent if:

$$s = \frac{2}{T}\frac{z-1}{z+1} \tag{25}$$

Where s is the Laplace variable. This is commonly known as the bilinear transform, or Tustin's method [8]. Note that the continuous transfer function is found by applying the Laplace transform to Eq. (19). It can further be shown that by approximating the integral of the continuous state space equations using the trapezium rule, the relationship between the discrete and continuous state matrices becomes:

$$\begin{aligned} A &= \frac{2}{T}(I + \hat{A})^{-1}(\hat{A} - 1) \\ B &= \frac{2}{\sqrt{T}}(I + \hat{A})^{-1}\hat{B} \\ C &= \frac{2}{\sqrt{T}}\hat{C}(I + \hat{A})^{-1} \\ D &= \hat{D} - \hat{C}(I + \hat{A})^{-1}\hat{B} \end{aligned} \tag{26}$$

A similar analogy could be drawn for the continuous-time case, where it can be shown that the continuous system frequency response is obtained when the poles are evaluated on the imaginary axis, namely:

$$s = i\omega_k \tag{27}$$

Substituting Eqs. (23) and (27) into (25), the nonlinear mapping between continuous and discrete frequency is derived:

$$\omega_k = \frac{2}{T}\tan\left(\frac{\omega_k^d}{2}\right) \tag{28}$$

For a more detailed discussion of the above relationships refer to [9–11].

This equivalency provides the basis for a system identification algorithm [6], which requires frequency response data on a set of *M+1* equispaced discrete frequencies between 0 and π. The equivalent continuous frequencies can then be used as inputs to the LFD solver and the output is both the continuous system frequency response and the equivalent discrete system frequency response. These results provide the necessary inputs to the system identification algorithm to identify a reduced order state space model.

The parameter T has an impact on the distribution of the continuous frequencies mapped from the equispaced discrete frequencies. A higher value gives more continuous frequencies close to zero, however using a very large sampling period also means that the system dynamics at higher frequencies is not fully captured. This is due to frequency warping as the spacing between the continuous frequencies increases at discrete frequency values closer to π. To overcome this, alternative methods to the trapezoidal mapping could be sought, which produce a nonlinear one to one mapping between continuous and discrete frequencies. Examples include Euler's forward or backward difference methods. For all cases in this study a value of $T = {}^{70}/_{2\pi}$ and $M = 2^8$ has been used, giving a total of $N_\omega = 257$ discrete frequencies from 0 to π. It has subsequently been shown that lower values of *M* also gives viable ROMs, thus further reducing the total required computational time.

The ROM generation process starts from a block Hankel matrix formed from the frequency responses [6]. Taking the SVD of this matrix, and partitioning the SVD matrix to separate the largest eigenvalues, a low-dimensional subspace of the SVD can be created. This is then used to find the discrete $\hat{A}$ & $\hat{C}$ matrices. The discrete $\hat{B}$ & $\hat{D}$ matrices are subsequently determined by solving a least squares problem to find the best fit to the given frequency response data. The continuous state matrices can then be determined from the discrete matrices using Eq. (26).

F. ROM testing

Both periodic and non-periodic test cases were considered in order to test the ROM. Various 1-cosine gust profiles were used as input to the reduced system, and the outputs were compared to the responses from 1-cosine gust inputs to the LTD solver. The same was also done for a step input, in the form of a sharp edged gust.

To find the response of the LTD solver to a 1-cosine vertical gust the following gust was prescribed:

$$v_g = \begin{cases} \frac{v_{g_{max}}}{2}\left(1 - \cos\left(\frac{2\pi}{\lambda}x_{g_0}\right)\right) & x_{g_0} \le 0 \quad \& \quad x_{g_1} \ge 0 \\ 0 & \text{Otherwise} \end{cases} \tag{29}$$

Where x_{g_0} & x_{g_1} are defined as:

$$\begin{aligned} x_{g_0} &= x - x_0 - u_{ref}t \\ x_{g_1} &= x_{g_0} + \lambda \end{aligned} \tag{30}$$

And x_0 denotes the gust starting position in the spatial grid.

To find the response of the ROM to the 1-cosine gust, the reduced continuous state matrices were re-discretised at a suitable sampling rate to ensure no frequency data is lost. This could be done by either using the inverse bilinear transform given by Eq. (31) below, or by using the principal of Zero Order Hold (ZOH), given by Eq. (32). For both methods very good agreement between the response from the ROM and the LTD was found.

$$\begin{aligned} \hat{A} &= \left(\frac{2}{T}I + A\right)\left(\frac{2}{T}I - A\right)^{-1} \\ \hat{B} &= \frac{2}{\sqrt{T}}\left(\frac{2}{T}I - A\right)^{-1}B \\ \hat{C} &= \frac{2}{\sqrt{T}}C\left(\frac{2}{T}I - A\right)^{-1} \\ \hat{D} &= D + C\left(\frac{2}{T}I - A\right)^{-1}B \end{aligned} \tag{31}$$

$$\hat{A} = e^{(AT)}$$
$$\hat{B} = \int_0^T e^{A\tau} B \, d\tau = A^{-1}(\hat{A} - I)B \tag{32}$$
$$\hat{C} = C$$
$$\hat{D} = D$$

The exponential term in Eq. (32) is evaluated using Padé scaling followed by squaring, which is the basis for the built in MATLAB exponential function.

Finally, the sharp edge gust profile used to obtain the step response is given by the following equation, where x_{g_0} is defined as in Eq. (30).

$$v_g = \begin{cases} v_{g_{max}} & x_{g_0} \leq 0 \\ 0 & x_{g_0} > 0 \end{cases} \tag{33}$$

Results for various Mach number, aerofoil, and gust profile combinations are given below.

III. Results

In order to validate the ROM for different flow regimes and aerofoils a number of test cases were chosen, which can be found in the table below.

Table 1. Test cases for different aerofoil & Mach number configurations

Case	Aerofoil	Mach Number
T1	NACA0006	0.85
T2 , T3	NACA0010	0.735 , 0.85
T4	NACA0018	0.25
T5 , T6	NACA2410	0.25 ,0.735

Euler C-grid meshes were constructed around each aerofoil with grid sizing of 181×60, with 100 cells on the aerofoil surface. As an illustration the grid for the NACA0010 aerofoil is displayed below.

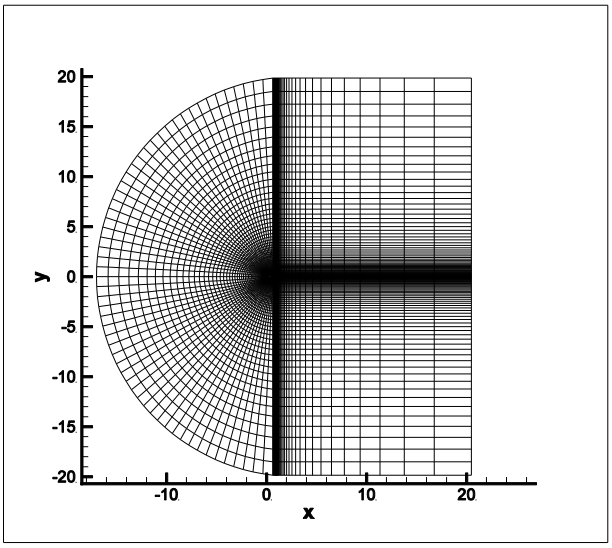

Figure 1. C-grid around NACA0010 aerofoil

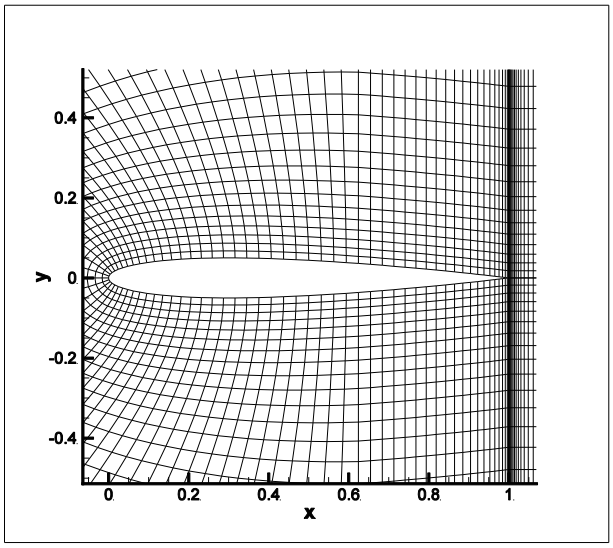

Figure 2. NACA0010 aerofoil surface grid

The graphs of the steady pressure distribution for each test case at zero incidence can be found in Figures 3-8:

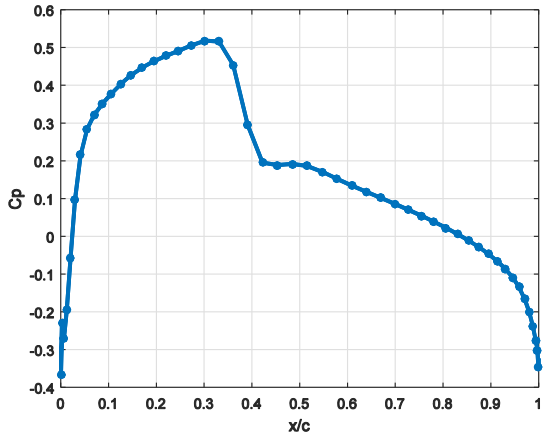

Figure 3. Steady pressure distribution case T1

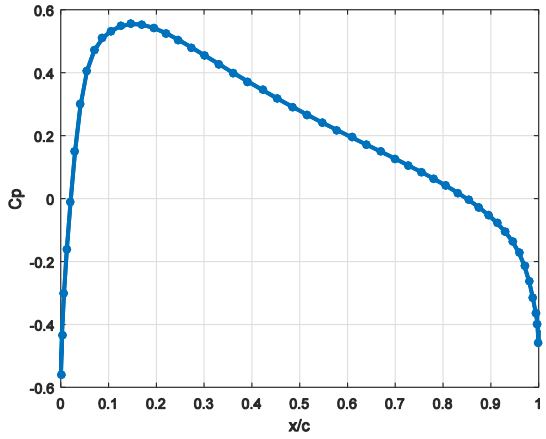

Figure 4. Steady pressure distribution case T2

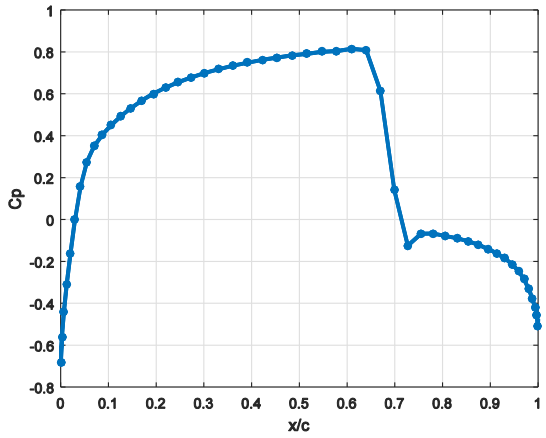

Figure 5. Steady pressure distribution case T3

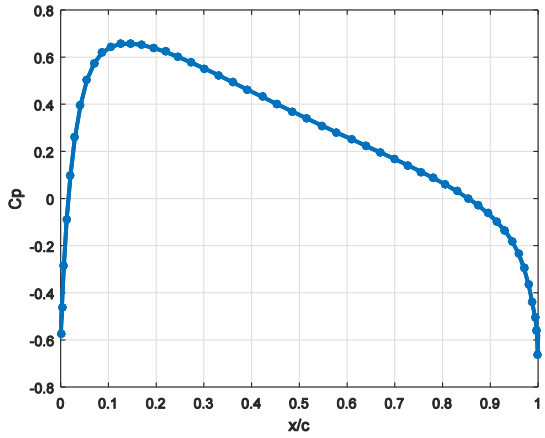

Figure 6. Steady pressure distribution case T4

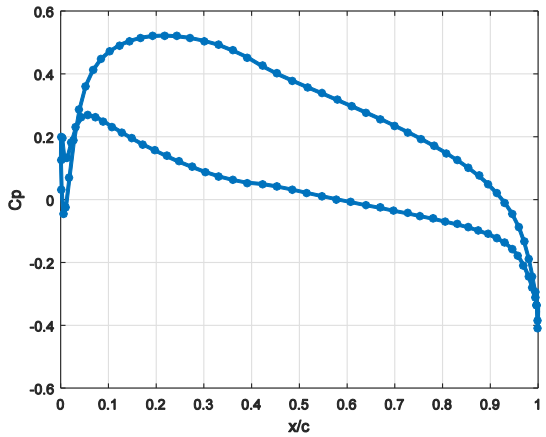

Figure 7. Steady pressure distribution case T5

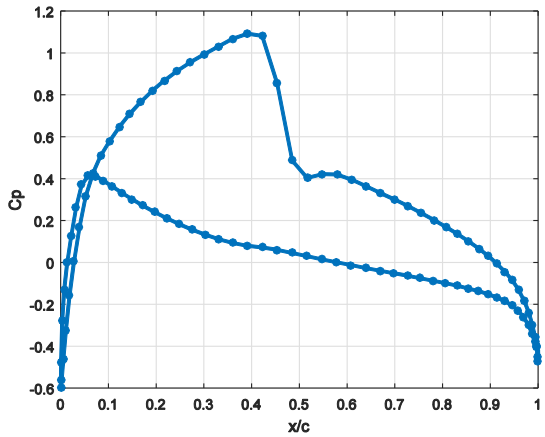

Figure 8. Steady pressure distribution case T6

As explained previously the LFD code is used to obtain the frequency response of the system, by prescribing gusts at discrete frequencies from 0 to π. The following results show a comparison between the frequency response using the frequency domain SVM and FVM solver, for the test cases T2 and T4.

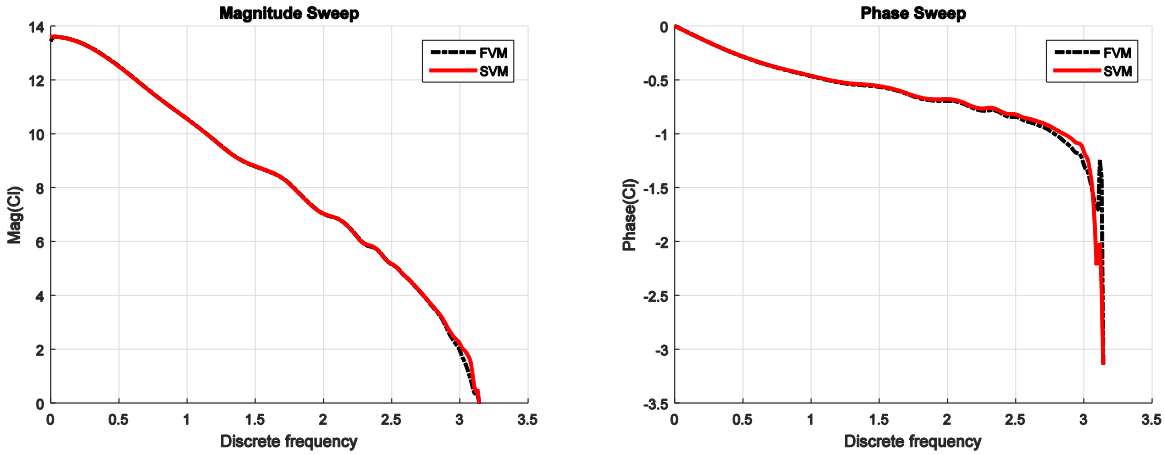

Figure 9. FVM vs SVM comparison of LFD results. Case T2

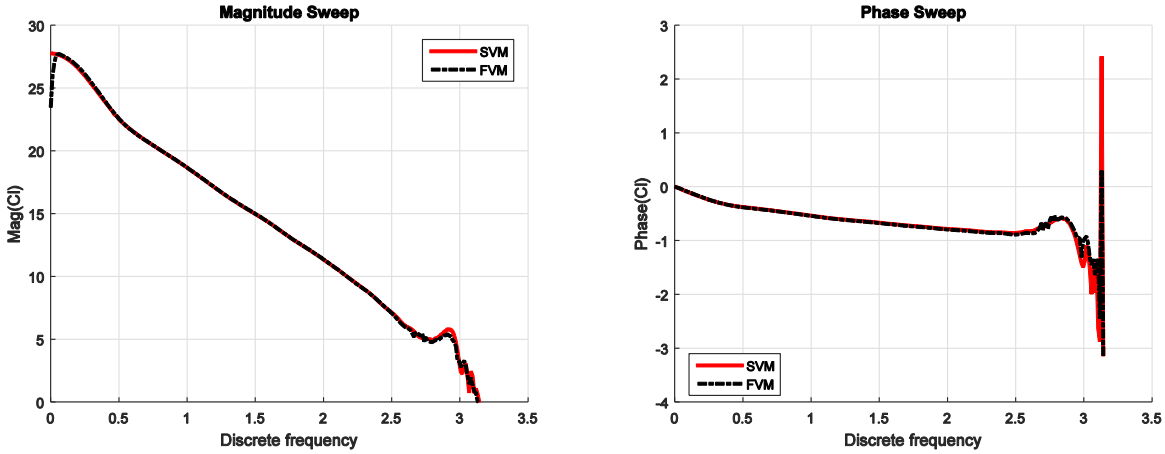

Figure 10. FVM vs SVM comparison of LFD results. Case T4

Using the frequency responses from the SVM solver, ROMs were constructed for the 6 test cases introduced earlier. Plots of the ROM frequency response versus the original system can be found below. The size of the reduced model, N_r, which determines the number of singular values of the block Hankel matrix used to construct the low-dimensional model, is indicated under the figure for each test case.

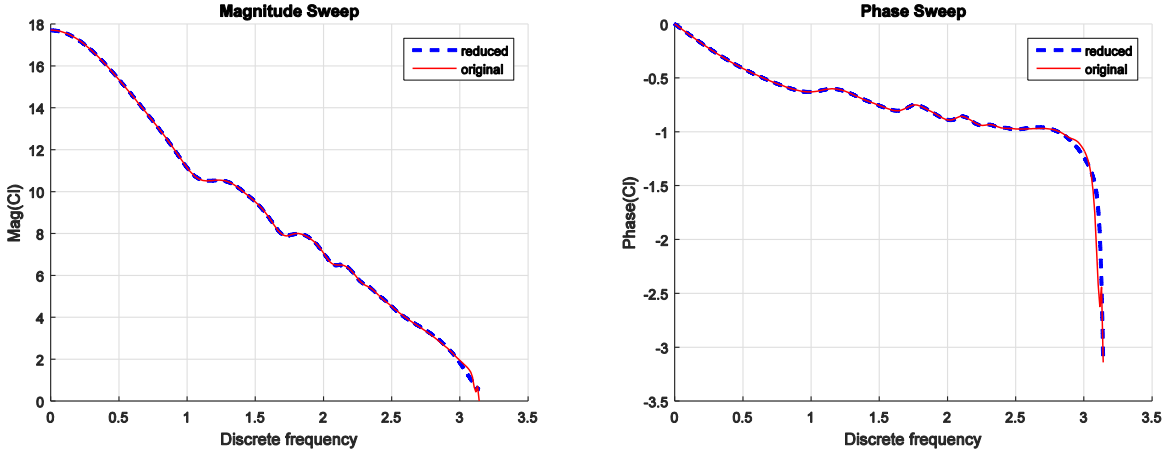

Figure 11. ROM case T1. Reduced system size = 25

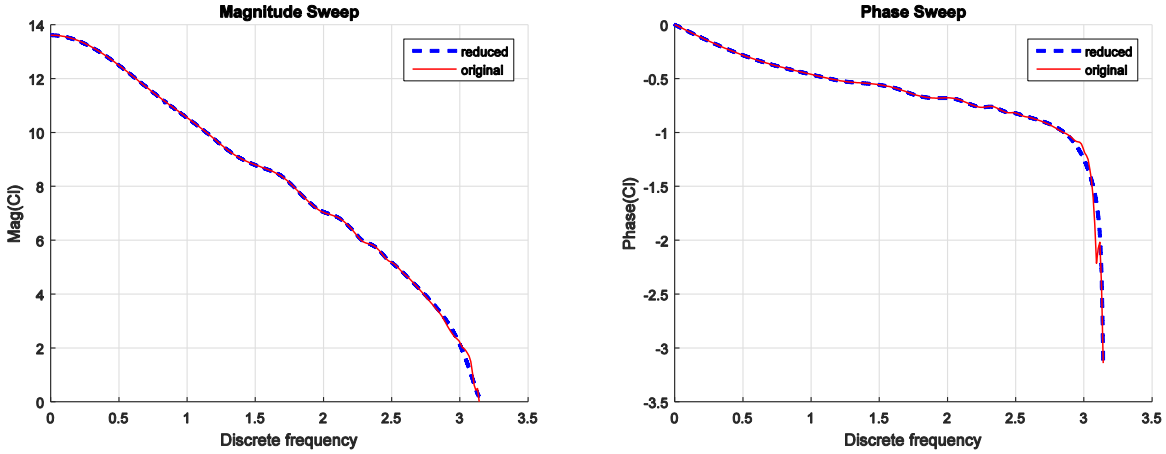

Figure 12. ROM case T2. Reduced system size = 25

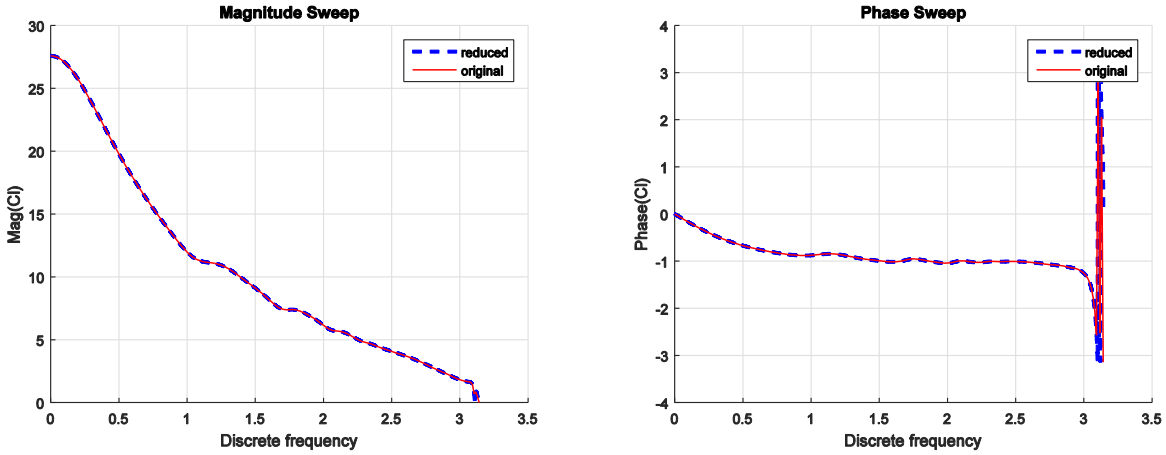

Figure 13. ROM case T3. Reduced system size = 25

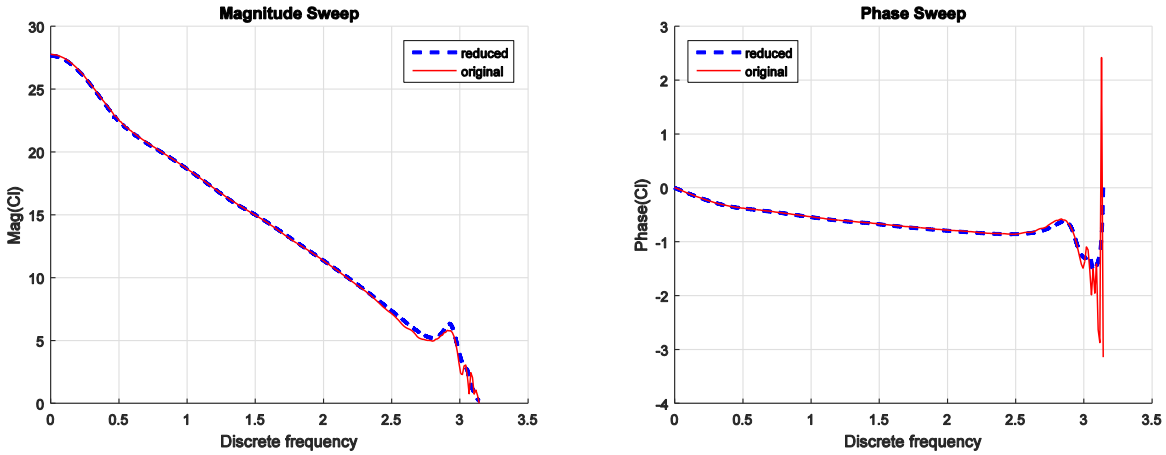

Figure 14. ROM case T4. Reduced system size = 25

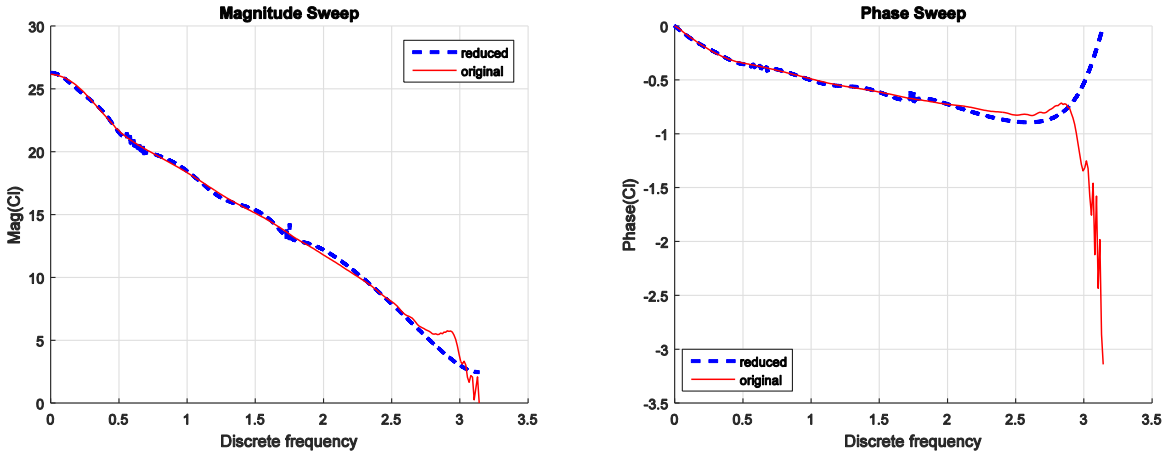

Figure 15. ROM case T5. Reduced system size = 25

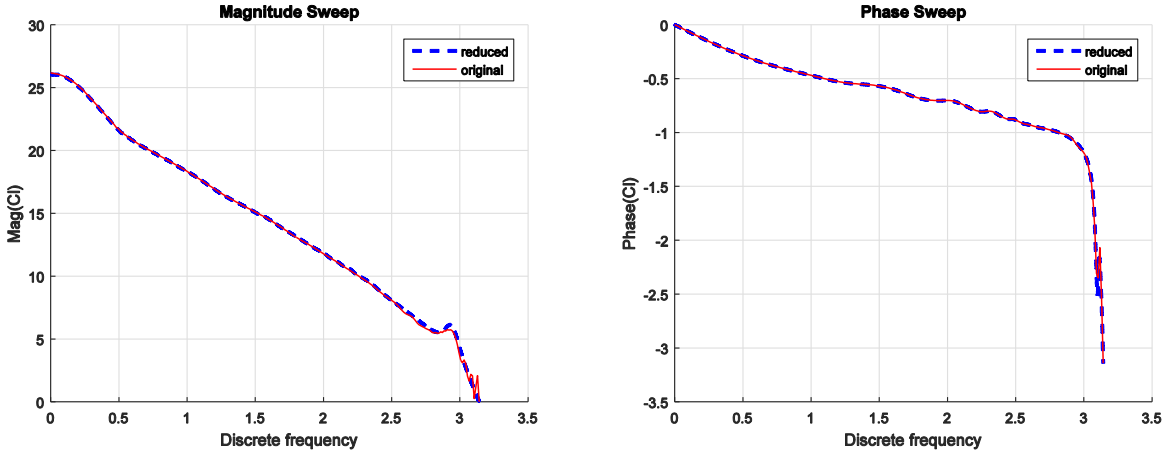

Figure 16. ROM case T5. Reduced system size = 55

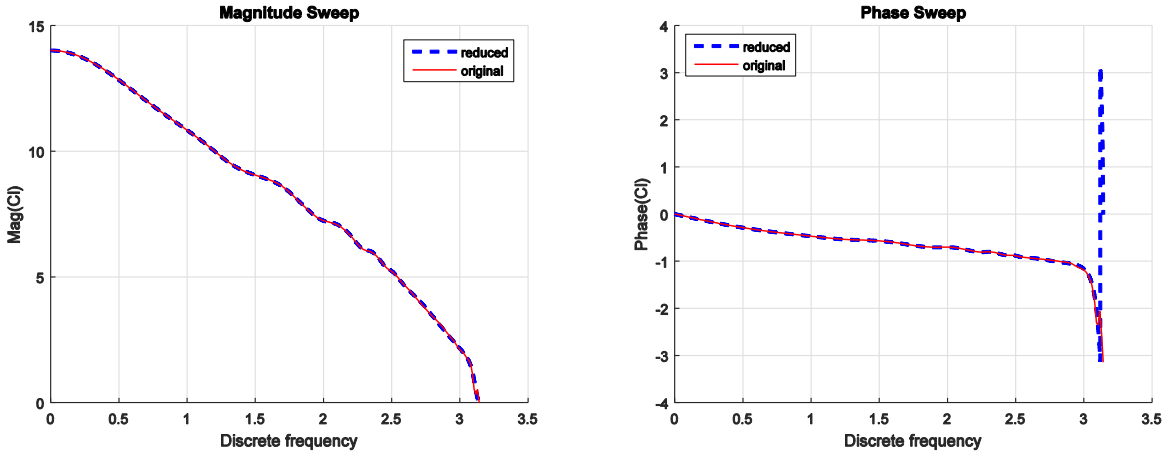

Figure 17. ROM case T6. Reduced system size = 25

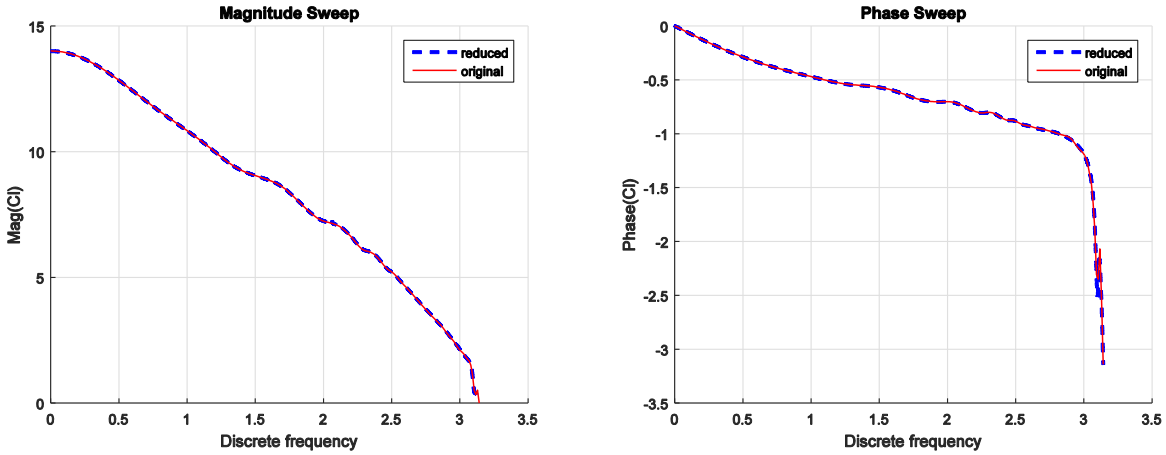

Figure 18. ROM case T6. Reduced system size = 35

Figures 11 to 14 show that for test cases T1 to T4, a reduced system size of 25 gives models that agree well with the original system, and that the frequency response is well-behaved at smaller frequencies. For cases T5 and T6, which both correspond to the asymmetric NACA2410 aerofoil, a ROM size of 25 gives rise to a reduced system which doesn't fully capture the dynamics of the original system. Figures 15 and 18 show that increasing the size of the reduced model ensures that the system dynamics, especially at higher frequencies, is captured. On the other hand, making the size of the reduced model overly large will over-fit the ROM to the original system which can cause issues with ROM behaviour.

As previously stated a total number of 257 frequencies were used to construct the system frequency response for each test case. A suitable ROM could still be created with a much smaller system. For instance, the figure below shows the ROM created for test case T2, using $N_\omega = 33$ data points, while setting the size of the reduced system to $N_r = 9$.

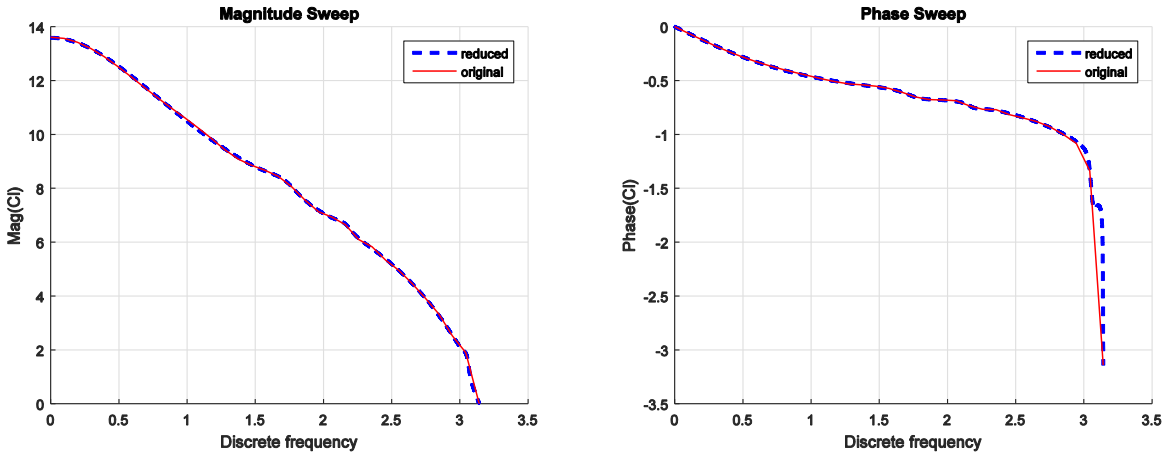

Figure 19. ROM case T2. Number of frequency samples 33, Reduced system size 9

In order to validate the ROMs obtained for the test cases chosen, a number of gust profiles were prescribed to both the reduced system, and the full LTD system, and the results were compared to verify the transient and steady state response of the ROM. The following table shows the gust cases chosen:

Table 2. Gust cases prescribed for comparing LTD results with ROM

Case	Gust Type	Gust length (in chords)	$\Delta\alpha_{eff}$ (deg)
G1	1-cosine	0.5	2
G2	1-cosine	1	2
G3	1-cosine	1	5
G4	1-cosine	10	5
G5	1-cosine	25	1
G6	Step (Sharp Edge)	NA	$v_{g_{max}} = 1$

The plots of the lift coefficient from applying gust cases G3 & G6 to all test cases in Table 1 are given below, where results from both the ROM and LTD solver are given for comparison. For configurations T5 and T6 with the cambered aerofoil the results for both ROM sizes are shown for each case.

Gust case G3 was chosen in order to test the ROM at higher frequencies, where there is some disagreement between the ROM and the linear time domain results. Results from other gust cases at lower frequencies are also included thereafter.

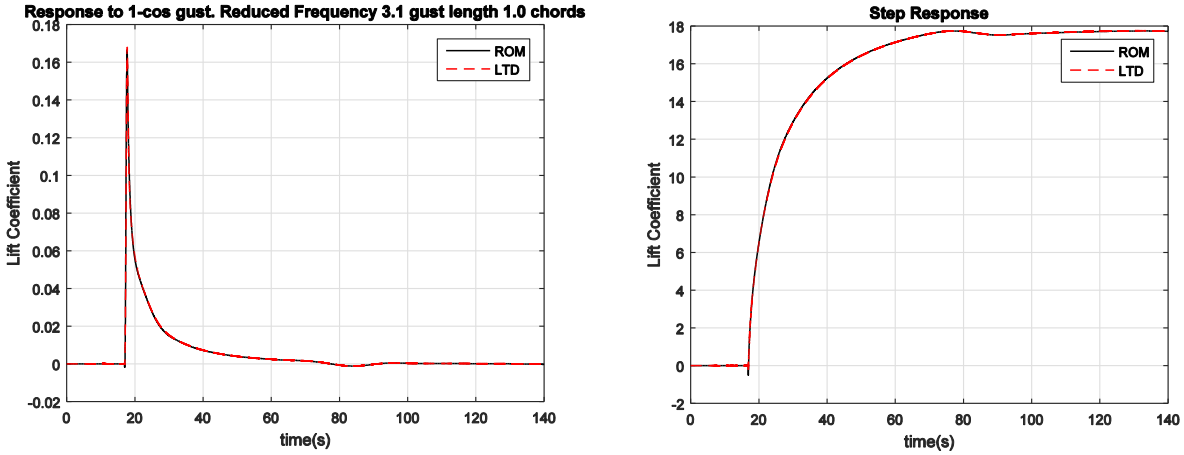

Figure 20. Response of test case T1 to gusts G3 and G6. Size of ROM Nr = 25

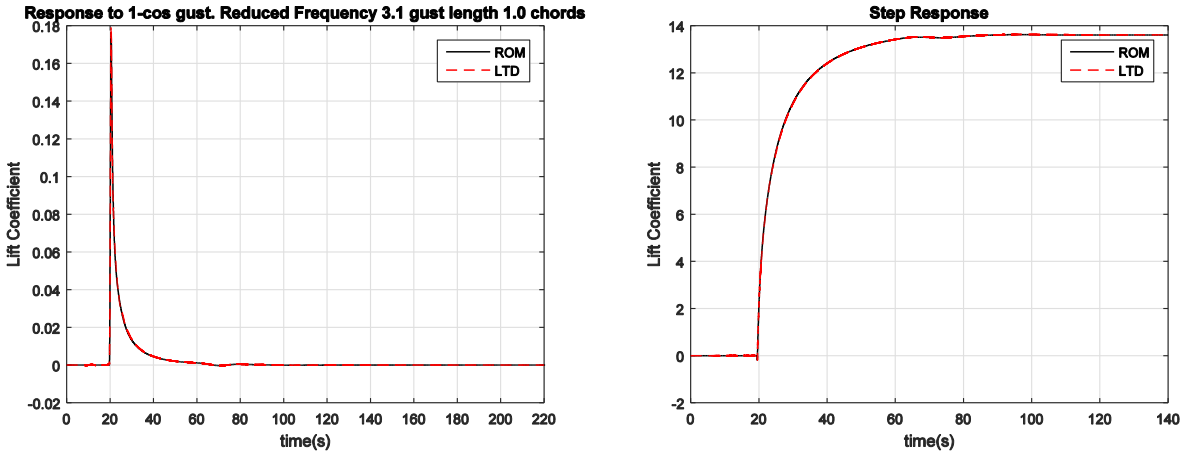

Figure 21. Response of test case T2 to gusts G3 and G6. Size of ROM Nr = 25

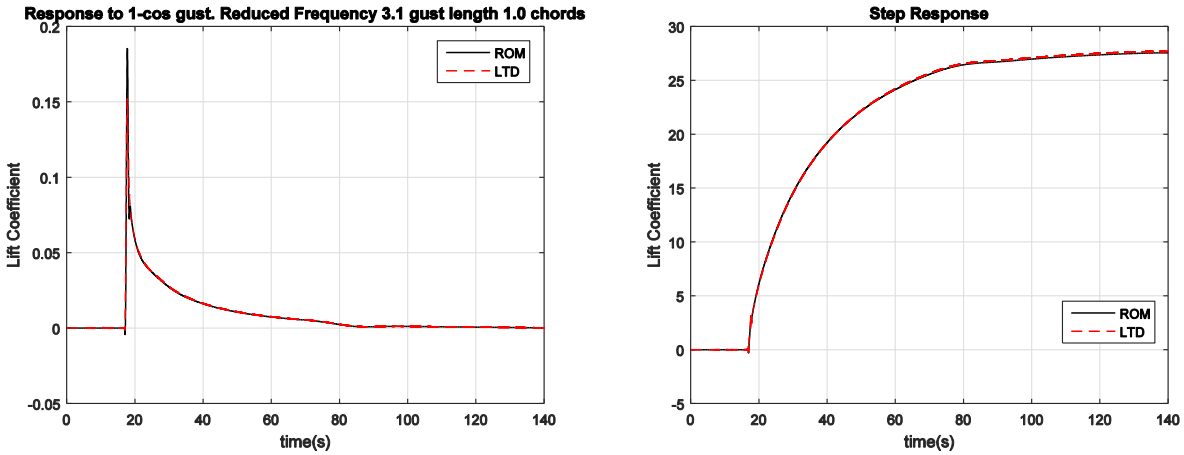

Figure 22. Response of test case T3 to gusts G3 and G6. Size of ROM Nr = 25

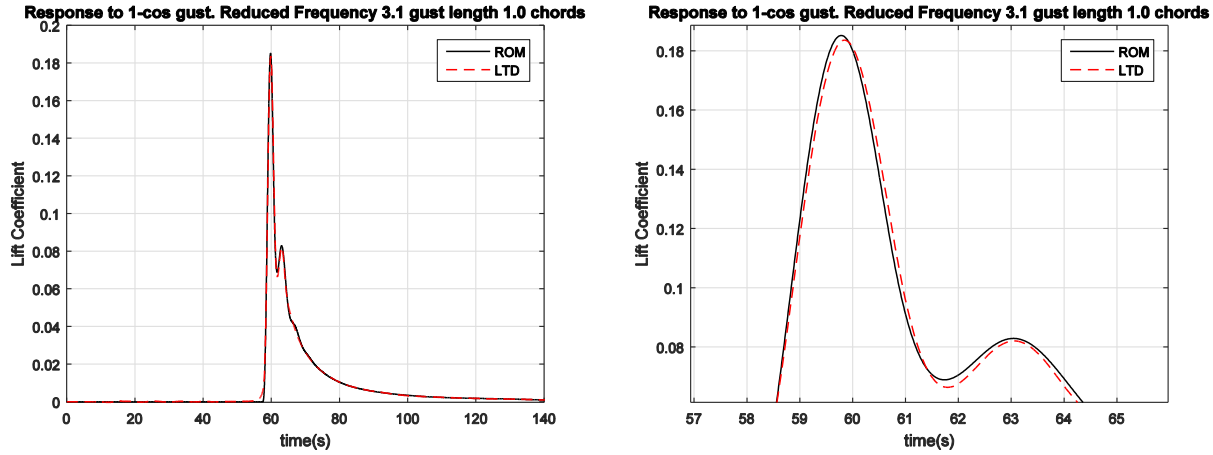

Figure 23. Response of test case T4 to gust G3. Size of ROM Nr = 25

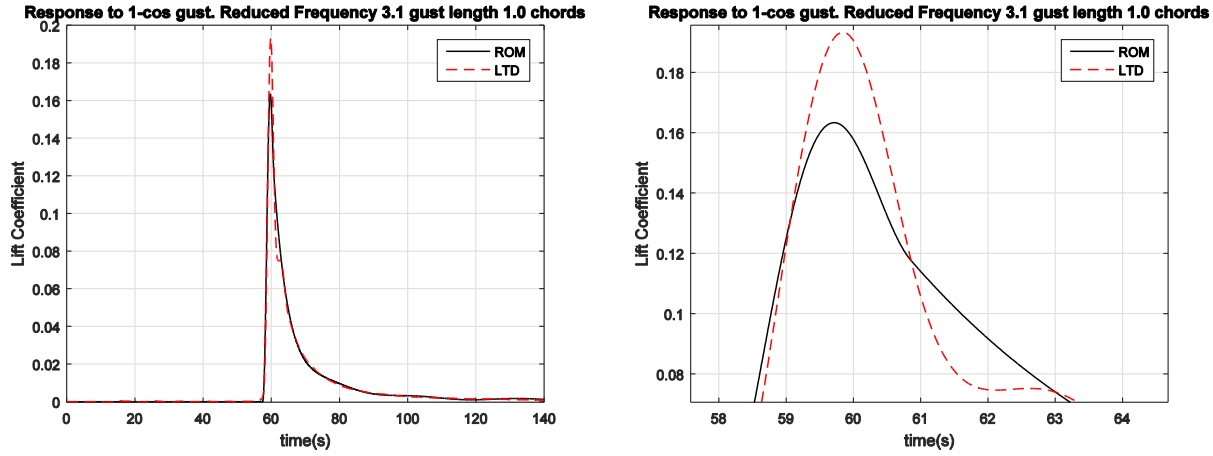

Figure 24. Response of test case T5 to gust G3. Size of ROM Nr = 25

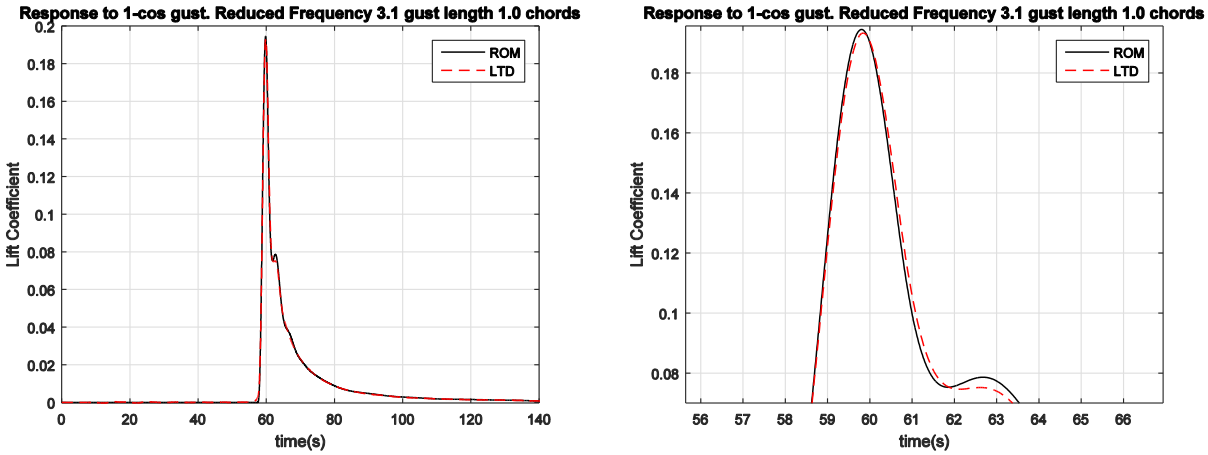

Figure 25. Response of test case T5 to gust G3. Size of ROM Nr = 55

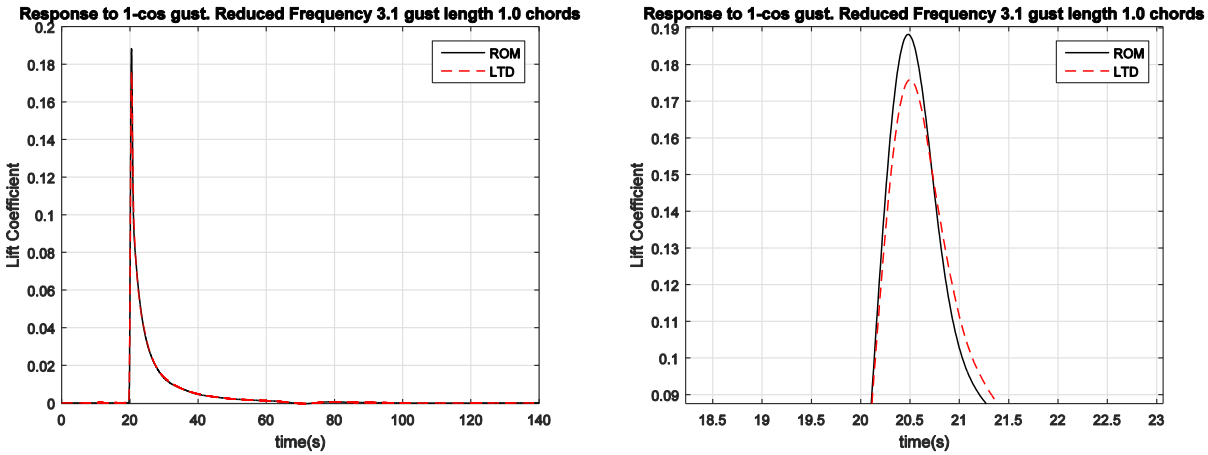

Figure 26. Response of test case T6 to gust G3. Size of ROM Nr = 25

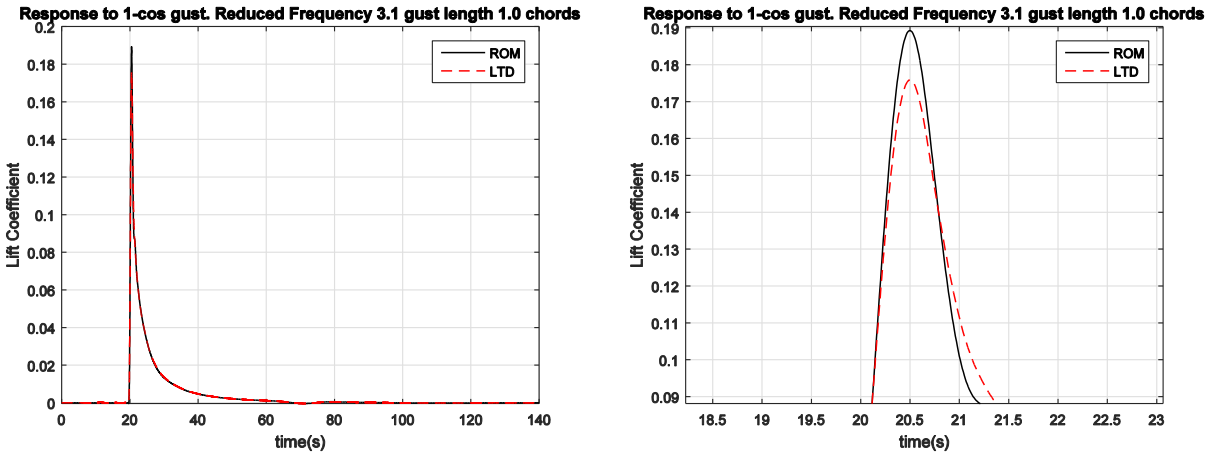

Figure 27. Response of test case T6 to gust G3. Size of ROM Nr=35

From Figures 22 and 23 it can be seen that for cases where the system dynamics is characterised by larger transients, increasing the size of the ROM produces results which are closer to those from the LTD solver, since this enables the dynamics to be captured fully. This is the case for the NACA0018 and NACA2410 aerofoils at Mach 0.25,

as it can be seen from Figures 21 and 22 that the time domain response exhibits some oscillatory behaviour after the gust peak. Figure 28 below shows the pitching moment response to the 1-cosine gust G3, of the NACA2410 aerofoil at Mach 0.25 and Mach 0.735 (*i.e.* test case T5 and T6), where the time has been non-dimensionalised with respect to gust impact time. The plot shows that the response at Mach 0.25 exhibits longer rise time, and has greater transients.

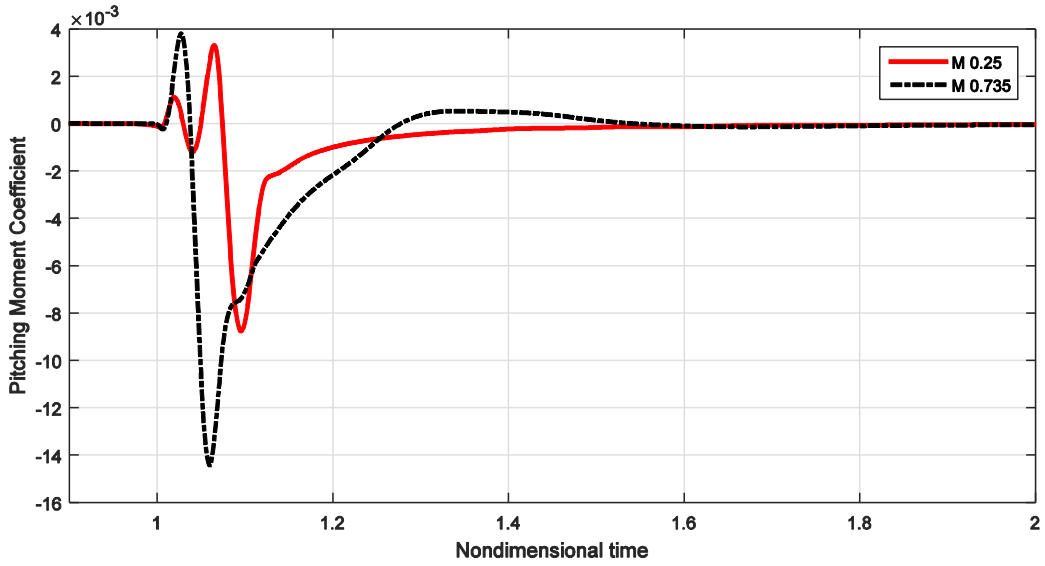

Figure 28. Pitching moment response of NACA2410 aerofoil to 1-cosine gust G3 (gust length= 1 chord, $\Delta\alpha_{eff}$ =5 deg)

As previously discussed, a smaller ROM was also created for test case T2, using $N_\omega = 33$ data points, with a reduced system size of $N_r = 9$. The response of this system to gust case G3 is shown below, where the response of the larger ROM is also added for comparison.

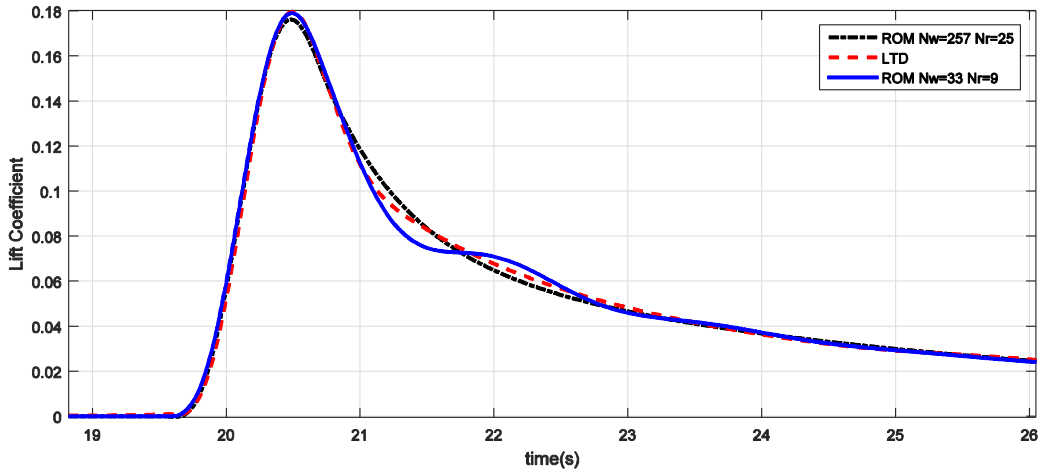

Figure 29. ROM size comparison for response of test case T2 to gust G3

It can be seen that the smaller ROM is better at matching the peak response of the LTD lift coefficient, however it also features additional oscillatory response as the lift coefficient settles back to 0.

Below are some results from inputting the other gust cases set out in Table 2 to the test cases from Table 1. For all the following cases the size of the ROM was set to 25, and the entire 257 frequencies were used to obtain the frequency response.

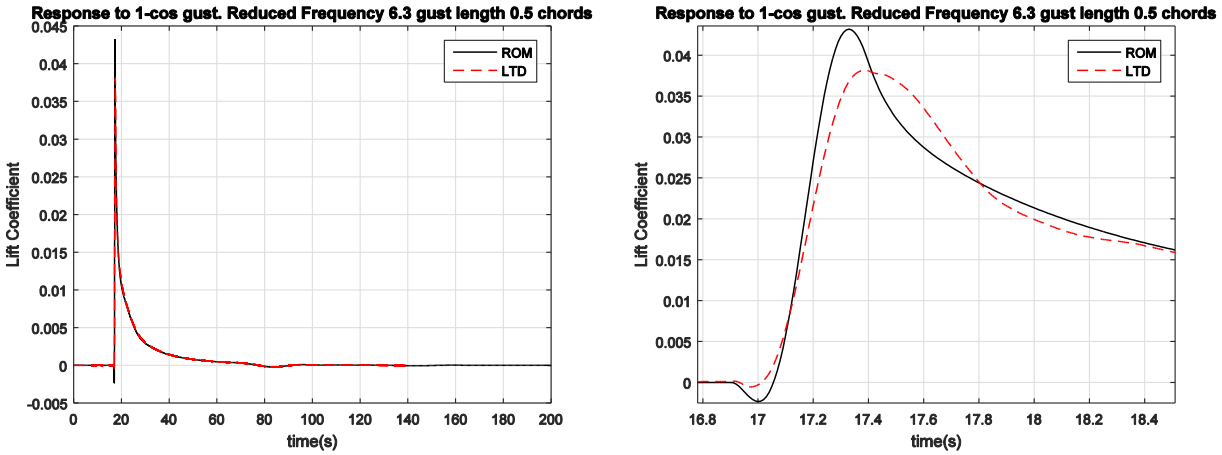

Figure 30. Response of case T1 to gust G1

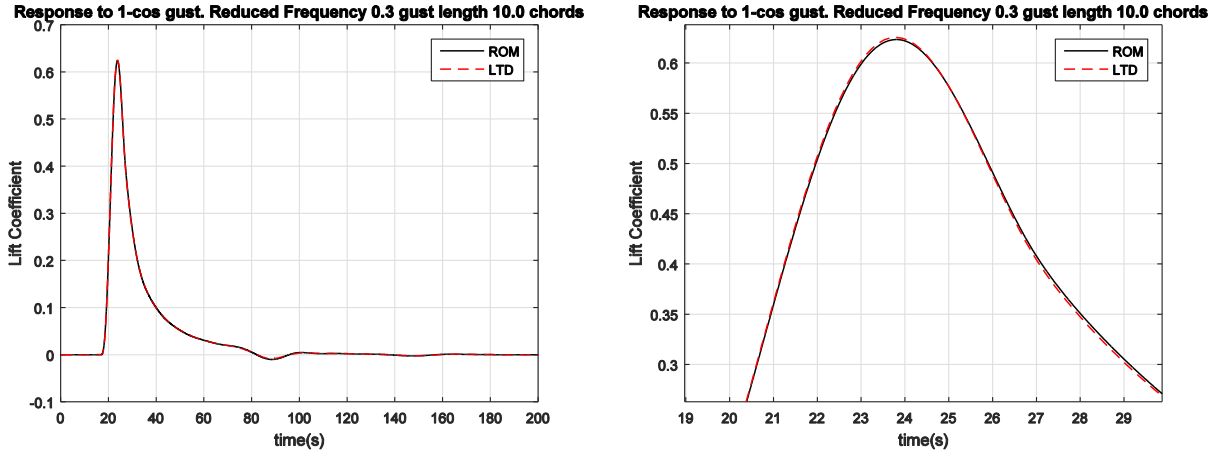

Figure 31. Response of case T1 to gust G4

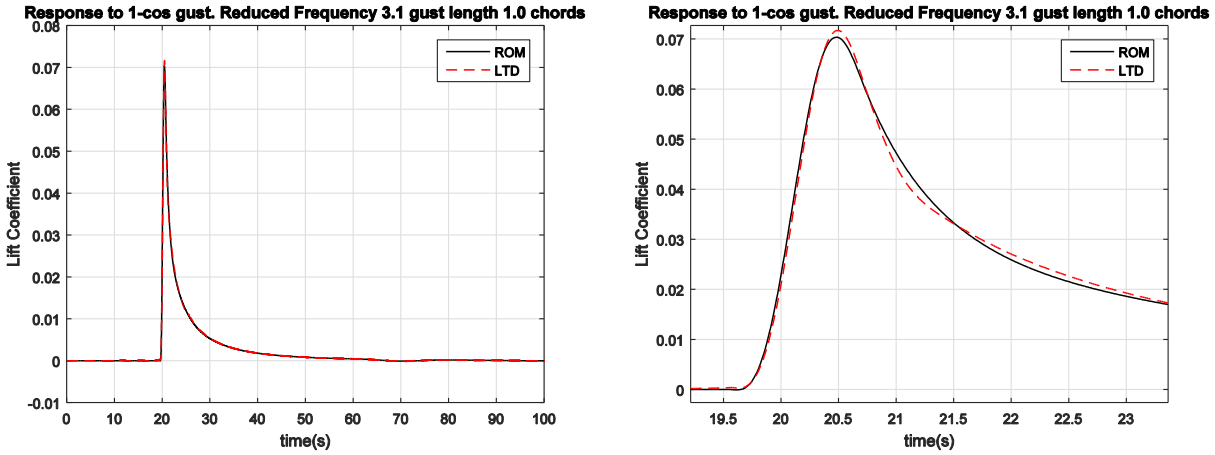

Figure 32. Response of case T2 to gust G2

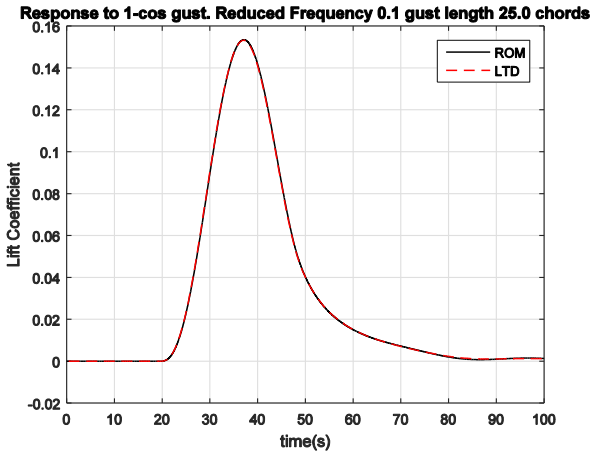

Figure 33. Response of case T2 to gust G5

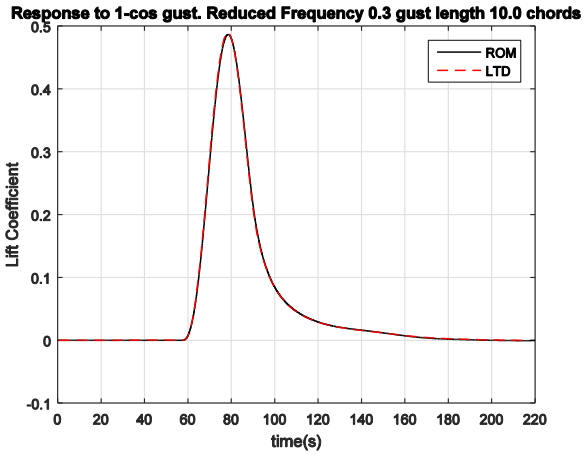

Figure 34. Response of case T4 to gust G4

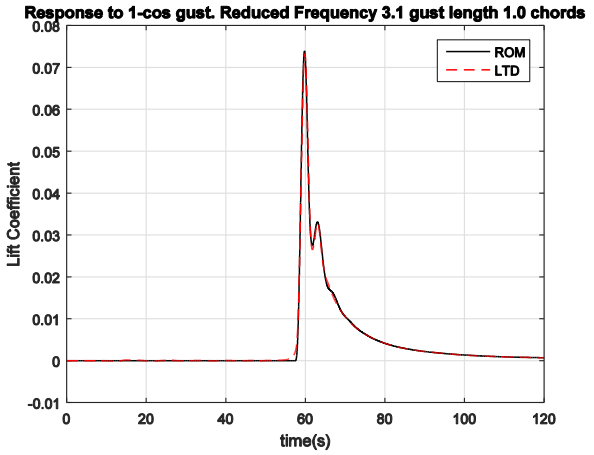

Figure 35. Response of case T4 to gust G2

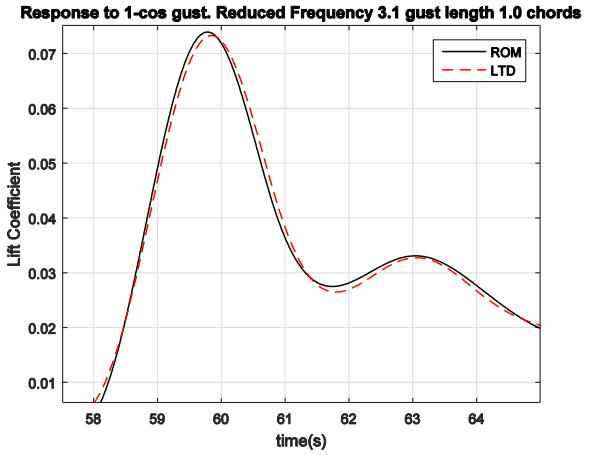

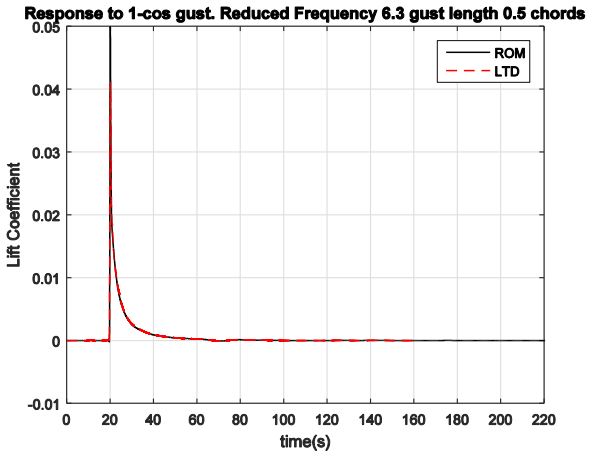

Figure 36. Response of case T6 to gust G1

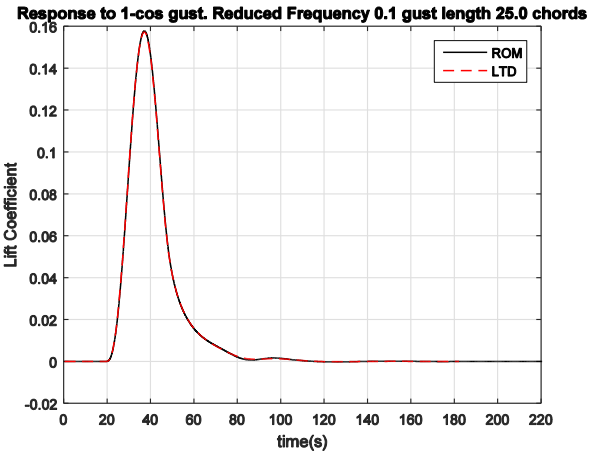

Figure 37. Response of case T6 to Gust G5

The figures show that the ROMs are generally better representative of the systems at lower frequencies, which is plausible given that more samples of the frequency response were concentrated closer to the lower frequencies, due to the choice of *T*. As discussed previously, a smaller value of *T* will concentrate more frequency samples towards the higher frequencies, at the cost of fewer samples near the lower frequencies. Moreover, it can be seen that the ROMs are consistently out by 1 time-step compared to the LTD results. This is due to the different time discretisation of the ROM and LTD solver.

IV. Conclusion

A reduced order model of a 2D rigid aerofoil-gust system has been constructed, using subspace based system identification to create models of lower dimension. The model is derived from the results of a linear frequency domain flow solver, and has the capacity to predict the output of the system to any given input, taking only a fraction of the time compared to running time-domain simulations. It has been shown that the model can predict the loads on the aerofoil very accurately at low excitation frequencies, while accurate high frequency predictions are also possible by using a higher sample rate.

Further research effort is being directed towards stabilising the reduced system frequency response via restarting if an unstable system has been identified. Further work is also being done to find methods to ensure the reduced system exactly matches the original system at zero input frequency, to ensure equal steady state gains.

Future work will include research into developing ROMs which can accurately model the nonlinearities arising in viscous transonic flow. The results found in this study and the analysis conducted on linear systems will provide the basis for creating the nonlinear models. Once fully developed the ROM can be used as a high fidelity computational tool for accurately predicting loads on a civil aircraft, while using minimal computational resources.

Acknowledgments

The research leading to these results was co-funded by Innovate UK, the UK's innovation agency, within the Enhanced Fidelity Transonic Wing project.

References

[1] Wales, C., Jones, D. P., and Gaitonde, A. L., "Prescribed Velocity Method for Simulation of Aerofoil Gust Responses," *Journal of Aircraft*, vol. 52, 2014, pp. 1–13.

[2] Thomas, P. D., and Lombard, C. K., "Geometric Conservation Law and Its Application to Flow Computations on Moving Grids," *AIAA Journal*, vol. 17, Oct. 1979, pp. 1030–1037.

[3] Singh, R., and Baeder, J., "Generalized moving gust response using CFD with application to airfoil-vortex interaction," *AIAA paper*, 1997, pp. 25–35.

[4] Bartels, R., "Developing an Accurate CFD Based Gust Model for the Truss Braced Wing Aircraft," *31st AIAA Applied Aerodynamics Conference*, 2013, pp. 1–15.

[5] Jameson, A., Schmidt, W., and Turkel, E., "Numerical solutions of the Euler equations by finite volume methods using Runge-Kutta time-stepping schemes," *AIAA paper*, 1981.

[6] McKelvey, T., Akçay, H., and Ljung, L., "Subspace-based multivariable system identification from frequency response data," *IEEE Transactions on Automatic Control*, vol. 41, 1996, pp. 960–979.

[7] Chen, C.-W., Juang, J.-N., and Lee, G., "Frequency Domain State-Space System Identification," *Journal of Vibration and Acoustics*, vol. 116, 1994, pp. 524–529.

[8] Oppenheim, A., Schafer, R., and Buck, J., *Discrete-Time Signal Processing*, New Jersey: Prentice-Hal Inc., 1998.

[9] Narayana, A., "State-space approach to the bilinear transformation and some extensions," *Education, IEEE Transactions on*, vol. 34, 1991, pp. 139–142.

[10] Shieh, L. S., Wang, H., and Yates, R. E., "Discrete-continuous model conversion," *Applied Mathematical Modelling*, vol. 4, 1980, pp. 449–455.

[11] Åström, K. J., and Murray, R. M., *Feedback Systems - An Introduction for Scientists and Engineers*, Princeton University Press, 2008.